Journal of Electroanalytical Chemistry 913 (2022) 116294

Contents lists available at ScienceDirect

Journal of Electroanalytical Chemistry

journal homepage: www.elsevier.com/locate/jelechem

Electrochemical evaluation of the grafting density of self-assembled monolayers of polyethylene glycol of different chain lengths formed by the *grafting to* approach under conditions close to the cloud point

Miriam Chávez, Guadalupe Sánchez-Obrero, Rafael Madueño, José Manuel Sevilla, Manuel Blázquez, Teresa Pineda *

Department of Physical Chemistry and Applied Thermodynamics, Institute of Fine Chemistry and Nanochemistry, University of Cordoba, Campus Rabanales, Ed. Marie Curie 2ª Planta, E-14014 Córdoba, Spain

ARTICLE INFO

Keywords:
Poly- ethylene glycol
Self-assembled monolayer
Grafting density
Cloud point
Reductive desorption

ABSTRACT

Grafting densities of polymers on gold surfaces are important parameters that inform about the chain conformation adopted by the chains, either mushroom or brush conformation. Most of the literature reports on this topic are based on ellipsometry measurements with other few results obtained from surface plasmon resonance or quartz crystal microbalance. In this work, we report the use of cyclic voltammetry of the reductive desorption (RD) process of mercapto-polyethylene glycol self-assembled monolayers (EGn-SAMs) to get the grafting densities of these polymers with different chain lengths (c.a. EG136, EG45 and EG18). When the EGn-SAMs are formed from aqueous solutions where the polymer chains are highly hydrated, an excess of charge density is obtained that apart from the capacitive contribution found in these processes, include an extra charge due to the hydrogen evolution reaction (HER) produced by the high ratio of water contained in the film that reduces concomitantly with the SAM RD process. However, preparing the EGn-SAM in the presence of high salt concentrations that lowers the water content within the chains, that is, using the cloud point strategy, very realistic grafting density values are obtained. The RD profiles of the EGn-SAMs completely change from a broad peak with high charge density to a structured peak that allows us the determination of grafting density values. Capacitance curves and the behavior of the electrochemical process of the $Fe(CN)_6^{3-/4-}$ redox pair in the presence of the films are also in agreement with the CV results. The grafting density values obtained by this methodology are higher than those reported for these SAMs by using other techniques but agree with the footprints expected for these chains when organized in a brush conformation. Moreover, they also are close to the values obtained by thermogravimetric analysis of the same films built on gold nanoparticles that behave as planar surfaces.

1. Introduction

Self-assembled monolayers of alkanethiols (C-SAMs) and oligo (ethylene glycol)-terminated alkanethiols (EG-C-SAMs) formed on noble metal surfaces have been widely studied because of their organized structures and capability to be tailored with different chemical functionalities in the exposed interface [1–4]. The fact that poly(ethylene glycol) (EGn) has demonstrated to prevent protein unspecific adsorption has stimulated great efforts in research dealing with the adsorption on different solid surfaces, through a strategy known as PEGylation [5], to make these surfaces biocompatible.

Most of the studies of biocompatibility have used EG-C-SAMs as model systems since the alkanethiol arm forces the organization of the whole molecule and adopting the EGn portion a helicoidal or all-trans conformation [6–11]. Thus, the influence of the number of EG moieties, the terminal group and the nature of the metal substrate have been studied to find out the origin of the biocompatibility of these films. However, most of the PEGylated surfaces used in biological systems are built with EGn chains devoid of the alkane arm, and most frequently with larger EGn than those used in the model studies. Thus, knowledge on the organization of these layers is still necessary to get more insight into the actual structure when EGn is directly attached to metal surfaces. One of the most important parameters in

* Corresponding author.
E-mail address: tpineda@uco.es (T. Pineda).

https://doi.org/10.1016/j.jelechem.2022.116294
Received 18 February 2022; Received in revised form 4 April 2022; Accepted 5 April 2022
Available online 8 April 2022

the characterization of these polymer films is the grafting density (σ) as it will define if the chains are in more or less extended conformations. In this sense, EGn hydration is an important factor determining the structure and the values of the σ parameter [12]. At lower σ, the chains are well hydrated and adopt the mushroom conformation whereas at higher σ values, the chains stretch away from the surface leading to the loss of hydration, and the brush regime is reached.

Grafting densities of EGn polymers on gold surfaces have been determined by using different experimental techniques and protocols. Upon decreasing EGn solubility by either increasing temperature or ionic strength, higher surfaces coverages are obtained [13]. Ex situ ellipsometry and neutron reflectometry techniques were first used to obtain σ values of EGn-SH molecules (with n from 18 to 120) on gold surfaces, that resulted higher than the theoretically calculated for the unperturbed chains under high- and low-solubility conditions. The driving force for chemisorption through the thiol group was considered to be sufficient for the coverage to proceed beyond the close-packed mushroom regime, forcing the chains to adopt an extended brush conformation [13].

The major problem found for the grafting of polymer chains to a surface starts when the binding reaches saturation because the overlap of coils. This overlapping occurs when the distance between grafting points is comparable to the coil size in solution [14,15]. One of the most useful approaches for increasing the σ values of polymers is to use dispersions where the individual coils are shrunk. This can be reached by using either less favorable solvents [16], or under polymer melt conditions [17,18], or by the "cloud point" grafting strategy [16]. Thus, the grafting process of EGn polymers in 0.9 M Na_2SO_4 at room temperature results in well-defined brushes of high density, and this is explained as due to an osmotic balance that, in the presence of salt, makes the polymer shrinks and more coils can then fit on the surface [19]. The height of these brushes, prepared with EGn of molecular weights from 2 to 30 kDa, agrees with the calculated values based on a model similar to the "de Gennes" [20] for strongly stretched brushes in which the height is proportional to the molecular weight [19]. Recently, Ortiz et al. [21] have verified this strategy by controlling the grafting density under different salt concentrations and found that the highest value is obtained when the EGn film is formed in the presence of 0.9 M Na_2SO_4 aqueous solution, and observed the conformational transition from mushroom to brush only when the grafting process proceeded during long periods, emphasizing the importance of adsorption time to obtain high σ and the brush conformation.

The *grafting to* approach for attaching polymer chains with a terminal thiol group on a gold surface follows the self-assembly strategy consisting in contact the metal surface with a solution of the thiol derivative for a determined time. This procedure readily produces SAMs of the polymer due to the main interaction of the thiol group with the gold surface atoms. One important parameter of these SAMs is the surface coverage (or σ) and, therefore, the footprint of the molecules. The literature on this topic reports the determination of these parameters as well as the thickness of the EGn films by using experimental techniques such as quartz crystal microbalance (QCM) and surface plasmon resonance (SPR) [19,21], and ellipsometry [13,17,22]. However, the strategy to obtain SAM surface coverages by using electrochemical techniques, has not yet been reported por this kind of systems. In this sense, the reductive desorption (RD) process of the SAM is a tool that gives this information based on the following reaction [23]:

$RS_{(ads)} + ne^- + xH_2O \rightarrow RS^{n-}_{(aq)} + xH_2O_{(ads)}$ (1).

where (*ads*) and (*aq*) refer to thiols in chemisorbed and solvated states, respectively. The reaction (1) is a solvent substitution reaction and, although for years has been treated as monoelectronic, is now accepted that this assumption depends on the specific system and the experimental conditions considered [24].

Pioneering work of Porter et al. [25] described the RD process of alkanethiol SAMs as a tool to determine desorption potentials and surface coverages. This desorption potential was found to depend on the chain length and the intermolecular interactions that are also related to the chain lengths [24,26]. The RD process as studied by cyclic voltammetry (CV) on a gold single crystal electrode is usually observed as a single peak whose charge density accounts for the reduction of the R-S-Au bond taking into account the reaction (1). Moreover, it is also believed that the overall charge density contains a capacitive current that has been determined as a 20 % of the total charge density measured [27–29].

When polycrystalline or polyoriented gold electrodes are used, a set of peaks are obtained for the RD process that are mainly ascribed to the desorption of SAMs patches attached to the different gold facets present in these electrode surfaces [30–34]. Nonetheless, there are some cases in which multi-wave voltammetry has been also observed in the RD of SAMs of long alkanethiols in Au(1 1 1) single crystal electrodes. These multi-wave voltammetric signals have been suggested to be due to the sequential desorption from sites with different binding energies [33,34], monolayer domains with different sizes and stability [35], and depletion micelles that are formed in the double layer region [33,36–38]. By using second harmonic generation (SHG) combined with cyclic voltammetry, Buck et al. [24] have proposed the intermolecular interactions as the origin of multi-wave behavior in *n*-alkanethiol desorption from single crystal surfaces. The double peak found for alkanethiols of intermediate lengths cannot be explained by a separation of capacitive and faradaic contributions as it was previously stated [37]. These two contributions are not separated and occurs through all the desorption process whenever the desorbed molecules remain at the interface, and the peak splitting is a consequence of the relative importance of the molecular interactions.

In the present work, we studied the RD processes of EGn-SAMs (with n = 18, 45 and 136) formed by the *grafting to* method on polyoriented gold (PO) and Au(1 1 1) single crystal electrodes by the cyclic voltammetry technique. We find that the charge density of the RD peaks obtained for the SAMs formed from EGn water solutions are higher than the expected for compact SAMs. However, the formation of these SAMs in the presence of high sodium phosphate (NaPi) concentrations (close to the EGn cloud point, i.e. under θ-conditions) gives results that allows us to determine more realistic σ values.

2. Experimental section

2.1. Materials.

Poly(ethylene glycol) methyl thiol of MW 800, 2000 and 6000 (EGn, n = 18, 45 and 136) were purchased from Sigma. The rest of the reagents were from Merck analytical grade. All solutions were prepared with deionized ultrapure water produced by a Millipore system.

The EGn solutions used for the grafting experiments were prepared by mixing the polymers with water or NaPi aqueous solutions. Different concentrations of salt were prepared to estimate the cloud points for the different polymers as defined by the initiation of phase separation (Figure S1).

The polymers were grafted to the gold surfaces by immersing the clean electrodes in the different polymer solutions and left overnight for surface modification at room temperature. Thereafter, the electrodes were thoroughly washed with water and dried with a N_2 flow.

2.2. Experimental methods.

Electrochemical experiments were performed on an Autolab (Ecochemie model Pgstat 30) instrument attached to a PC with proper software (GPES and FRA) for the total control of the experiments and data acquisition. A conventional three electrode glass cell comprising a platinum coil as counter electrode, a 50 mM KCl calomel (CE 50 mM) as reference electrode and either a polyoriented (PO) or an (1 1 1) single crystal gold (Au(1 1 1)), as the working electrodes, was

used. The PO gold electrode was a homemade sphere obtained by melting a gold wire up to reach a diameter of approximately 2 mm, attached to a gold wire that serves as electrode connection. The Au (1 1 1) single crystal was a cylinder of 3-mm diameter and 2 mm thick from Metal Crystals and Oxides Ltd., Cambridge, England, with a polished side. A gold wire mounted at its far tip, allowed easier handling of the crystal. Before each electrochemical measurement, the electrodes were annealed in a small Bunsen burner to light red melt for about 20 s and, after a short period of cooling in air, quenched in ultrapure water. The electrode was then transferred into the electrochemical cell with a droplet of water adhering to it to prevent contamination. The surface condition was confirmed by a cyclic voltammogram in 0.01 $HClO_4$, and the real surface area was determined from the gold oxide reduction peak obtained under these conditions (A(PO gold) = 0.24 cm^2; A(Au(1 1 1) = 0.07 cm^2).

The cyclic voltammograms for the reductive desorption processes were recorded in KOH 0.1 M solutions and these for the evaluation of the electron transfer in aqueous solutions were of 0. 1 M KNO_3 in the presence of $[Fe(CN)_6]^{3-/4-}$ 1 mM in each component. The electrochemical impedance spectroscopy measurements were obtained at the midpoint potential of the cyclic voltammogram registered for the naked electrode (at 0.08 V), using an amplitude rms of 10 mV and a frequency interval from 0.1 to 10000 Hz.

XPS analysis was performed using an MCD SPECS Phoibos 150 spectrometer (from the Servicio Central de Apoyo a la Investigación (SCAI) of the Universidad de Cordoba) employing non-monochromatized (12 kV, 300 W) Mg Kα radiation (1253.6 eV). The substrate, either clean or modified, was mounted on a steel sample holder and transferred to the XPS analytical chamber. The working pressure was less than $5{\cdot}10^{-9}$ Pa. The spectra were collected using a take-off angle of 45° respect to the sample surface plane. The spectrometer was calibrated by the binding energy (BE) of the Au $4f_{7/2}$ line at 84.0 eV. The standard deviation for the BE values was 0.2 eV. Survey scans were run in the 0–1100 eV range (pass energy 60 eV), and higher resolution scans were recorded for the C 1 s, O 1 s and S 2p regions. The analysis involved Shirley background subtraction, and whenever necessary, spectral deconvolution was carried out by nonlinear least-squares curve fitting adopting a Gaussian sum function, employing the software CASA-XPS.

Contact Angle (CA) Measurements were conducted by using an Optical Tensiometer Theta T200 device (Attension, Biolin Scientific) equipped with a high-speed camera (420 fps). The CAs of the formed SAMs were measured in sessile drop method. The experiments were performed at room temperature and at open atmosphere. The results are given as an average of six measurements.

3. Results and discussion.

The grafting of the polymer chains on the gold substrates was carried out as described in the experimental section. The films prepared overnight showed the best electrochemical performance and reproducible results and, therefore, this modification time has been chosen for the experiments. These EGn-SAMs are characterized by cyclic voltammetry (CV) following a potential program that allows to record the RD process. Thus, the EGn-SAM electrode is contacted with the electrolyte solution under potential controlled conditions at a value where the film is stable and, when the equilibrium is reached, the voltammetric curve is recorded. The RD process of the EG136-SAM formed on a poly-oriented (PO) gold electrode from a solution of EG136 0.18 mM in water is plotted in Fig. 1. The CV shows a broad reductive peak at −1.01 V (width at half height = 72 mV) that involves a charge density of 115 μC/cm^2. This charge density is too high to explain the desorption of an EG136-SAM even considering that the packing density is similar to that of alkanethiols (this process involves a charge density of around 70 μC/cm^2) [39]. Unexpectedly,

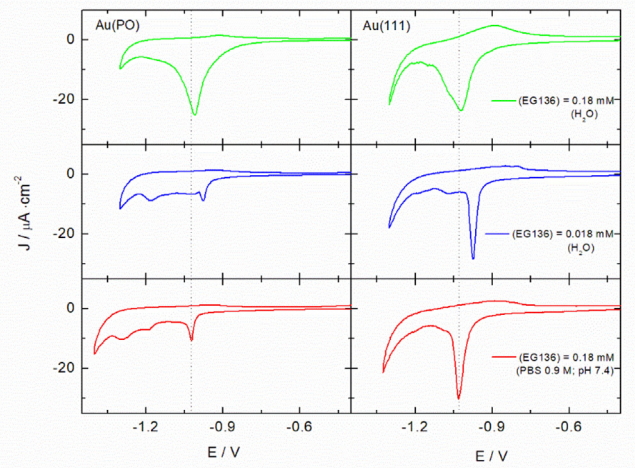

Fig. 1. CVs for the RD process of the EG136-SAM at PO and Au(1 1 1) electrodes formed in solutions of different EG136 concentrations and in the absence and presence of NaPi salt; v = 0.02 V/s.

the RD of the EG136-SAM formed under the same experimental conditions but using a single crystal Au(1 1 1) electrode also shows a broad peak (width at half height = 90 mV) slightly displaced in potential at −1.02 V (Fig. 1). Most of the RD peaks obtained from SAMs composed of alkanethiols or other mercaptoderivatives built at Au(1 1 1) surfaces appear as a sharp peak at the highest potential within these included in the sometimes resolved broad peaks obtained at polycrystalline gold electrodes. Moreover, using PO gold electrodes, a set of discrete peaks, being the first one ascribed to the desorption from (1 1 1) facets, is frequently observed [30,31,40]. The above results intrigue us for the following three reasons: the excess of charge density, the lack of discreteness of the peaks in PO electrode and the much broader peak in Au(1 1 1) electrode.

To get more insight into the origin of these features we have carried out experiments using different concentrations of EG136 in the SAM forming solutions. Whereas from 10 mM to the actual 0.18 mM EG136 concentrations the same behavior is observed, lowering the concentration to 0.018 mM, completely changes the RD profile. A set of peaks that remember the pattern obtained for EG7-SAM [31] in the PO gold electrode as well as a single sharp peak in the Au (1 1 1) electrode are now recorded (Fig. 1).

Higher charge densities than that corresponding to the RD of a complete monolayer obeying the reaction (1) have been previously found, and ascribed to the concomitant reduction of either R—S—S—R species that can be formed from free R-SH groups that remain into the SAMs or the reaction of the second thiol groups that are present in the form of intralayer disulfide bonds at the SAM interface when using dithiol derivatives [41–43]. In the case of EG136-SAM, the presence of free molecules in the polymeric film that are not able to reach the gold surface and complete the grafting reaction cannot be discarded at least in solutions of high concentrations. We have carried out XPS of these layers formed under these various experimental conditions and we have found that, in the case of the SAMs formed in solutions of the highest concentrations, a measurable ratio of either free S—H or disulfide exists in the layer (Figure S2). It is not expected that they correspond to disulfide species as the same phenomenon that impedes the diffusion of the chains to reach the gold surface or to leave the film, would also hinder the encounter of two chains in the film to form them. Thus, this extra contribution must be due to some free EG136-SH chains trapped into the film. However, the SAMs formed at lower EGn concentrations or in the presence of NaPi do not show that contribution.

In a study of RD of a homologous series of pyridine-terminated thiols with aromatic backbones in Au(1 1 1) electrodes, Rohwerder et al. [44,45] found multi-wave voltammetry with an extraordinary high reductive charge that gives unrealistic surface coverage values even if the non-Faradaic excess charges of around 20–30% due to the drastic change of capacity from the modified and unmodified substrate were taken into consideration [27,46–48]. They assigned this excess of charge to a parallel Faradaic reaction by noting that the RD process takes place within the H_2 evolution potential region and suggested that this reaction can occur concomitantly with the RD of the SAM at least when the potentials of the later become more negative as it was the case. Apparently, the RD process has a catalytic effect on the H_2 evolution reaction (HER) [44,45]. By combining experiments of CV, in situ ellipsometry, and hydrodynamic voltammetry, the concomitant oxidation of H_2 with the desorption of the monolayer is proposed. This rapid HER in respect to that taking place on a bare gold electrode, is thought to involve the orientation of water molecules in the gap created between the gold surface and the suspended reduced monolayer, accompanied by the diffusion of the positively charged electrolyte counter ions.

In our case, the EG136-SAMs formed from water solutions containing high EG136 concentrations should contain a high fraction of water. It is well known that the conformation of grafted chains on a surface depends on the chain density [13,49], and this is influenced by the actual conformation of the polymer in solution. As water is a good solvent for EGn polymers, they will be in a random coil conformation or unperturbed state where the polymer chains are interacting with water mainly by H-bonds. This conformation is transferred to the adsorbed state [12] and it is believed that the chains adopt the mushroom conformation that, on the other hand, supposes a low grafting density. Under these conditions the polymer layer contains a high ratio of water that can be reduced at the same potentials of the RD process. Thus, the water content in the SAM is high and it can be reduced in parallel with the SAM RD (Scheme 1). Only one peak appears in the voltammograms, in contrast to what happens with pyridine-terminated aromatic thiols that, after the consumption of the initially adsorbed water layer, water transport into inner plane requires to overcome the large electrolyte-blocking SAM domains and the catalyzed HER appears as a separated lower potential peak.

One necessary fact for this process to happen is that the molecular layer does not diffuse away from the surface, remaining at the interface forming patches or micelles. This can be the case for EG136 as shown in Figure S3. When the RD experiment is run starting at potentials of SAM stability and going to lower values up to the S-Au bonds are completely reduced, and then the scan continues to high potentials covering the oxidation of the gold surface atoms, the extra anodic charge obtained in respect to that of the oxidation of the gold surface, should correspond to the Au-S oxidation reaction [27,38]. A CV corresponding to the direct oxidation of a newly prepared EG136-SAM together with one for the bare electrode are also shown for comparison (Figure S3). The charge density recorded at high potentials is higher than that corresponding to the oxidation of the gold surface and lower than that involved in the oxidation of a complete monolayer. Thus, this is a confirmation that a great portion of the monolayer is retained at the electrode interface after the RD process.

This result can give the idea that the RD is not appropriate to determine the surface coverage of the polymer SAMs as we cannot separate the contribution of the rapid HER, if it is the case, from the actual RD charge density. However, it is well known that when the polymers are dissolved in poor solvents, the excluded volume expansion is reduced, and the chains adopt a more extended conformation (Scheme 1). Here, we use the method of changing the ionic strength of the EGn solutions by adding increasing concentrations of NaPi up to reach the solution cloud point. By using solutions of (EGn) = 0.17 mM, the cloud point in the presence of NaPi is determined for EG136, EG45 and EG18 that are the chains studied in this work. Whereas EG18 resists NaPi concentrations higher than 4 M without phase separation, EG45 and EG136 solution turbidity is produced at (NaPi) > 1.6 and 0.9 M, respectively.

When the RD of a EG136-SAM formed in a 0.9 M NaPi solution is recorded, a CV showing a set of well-defined peaks (Fig. 1, PO gold electrode) with a first sharp peak at −1.02 V that is displaced 40 mV more negative that the same peak for the SAM formed in a

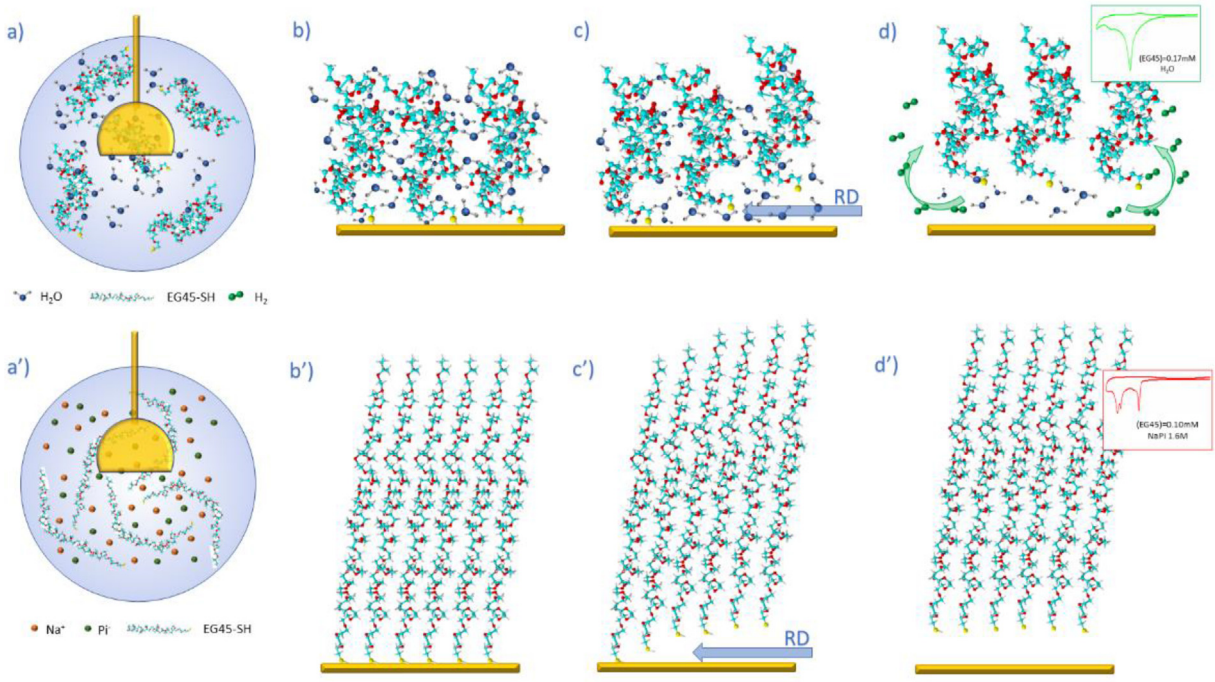

Scheme 1. Model for EGn-SAM formation and its reductive desorption process. Formation of the EGn-SAM in water (a) and under near cloud point conditions (a'); (b, b', c, c', d and d') the formed SAM is submitted to a potential scan to produce the reductive desorption process.

low EG136 concentration in the absence of salt is obtained. A similar behavior is observed for the RD from an Au(1 1 1) single crystal electrode. This effect is explained as a higher stability of the SAM formed from the high ionic strength solution in comparison to that formed in water.

Fig. 2 shows the CVs for the RD of EG136-SAMs formed in solutions of different salt concentrations. Increasing salt concentration, the shape of the CVs changes from the broad peak obtained in water to the multi-peak in the presence of salt. The charge density drastically decreases when adding salt to the formation solution and follows a smoothly increase up to 45 μC/cm^2 at higher salt concentrations.

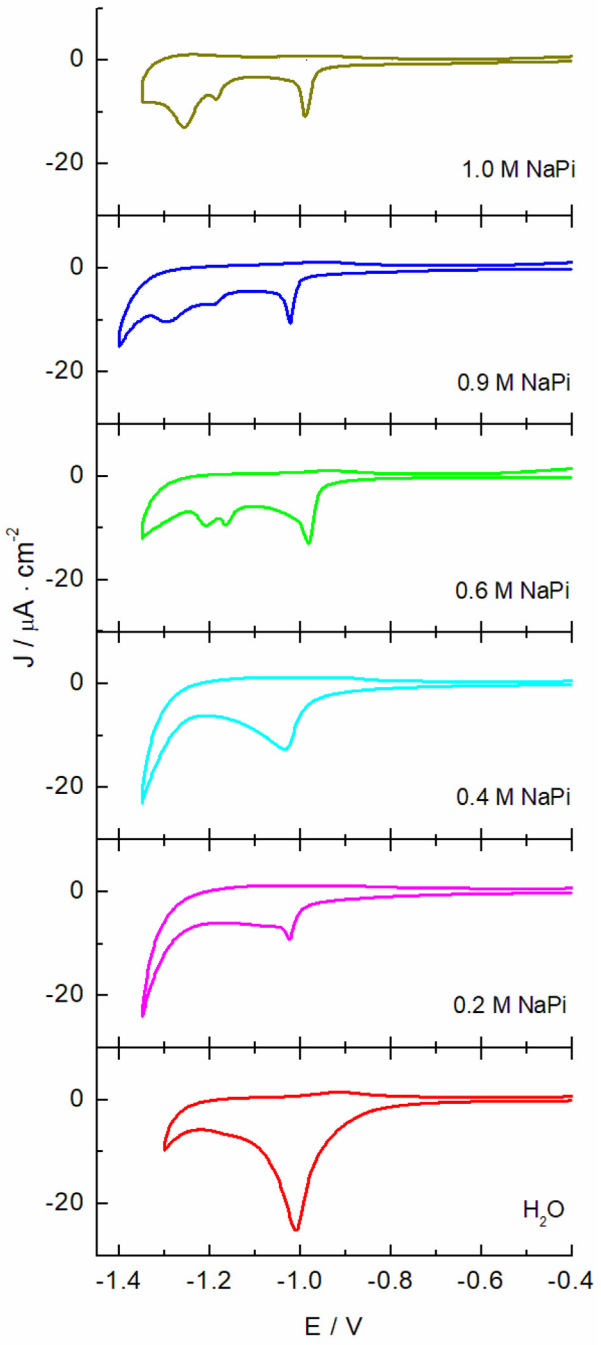

Fig. 2. CVs for the RD process of the EG136-SAM at PO electrodes formed in solutions of different NaPi salt concentrations; (EG136) = 0.18 mM; v = 0.02 V/s.

Concomitant with the changes in the RD profiles, the water contact angle values of the EG136-SAMs vary from 29.5 ± 5.2° to 36.1 ± 4.1° for the films formed in the absence and presence of salt (close to the cloud point), respectively. This is also an indication of the better organization of the molecules in the film exposing the terminal groups to the solution when the brush conformation is favored.

A similar behavior is obtained for the EG45-SAM Fig. 3. Whereas an excess of charge density together with an unresolved RD peak are obtained for the EG45-SAMs formed in water and in the presence of 0.9 M NaPi, a structured multi-peak curve is obtained when the SAM is formed in the presence of 1.6 M NaPi. The charge density obtained under these experimental conditions is of 46.5 μC/cm^2. Again, the CV recorded for the EG45-SAM prepared in a diluted water solution shows the multipeak pattern although the charge density is too low, indicating the formation of a partial monolayer.

In the case of EG18-SAMs, the multi-peak curves are recorded for the SAM formed in water as well as in the presence of 4 M NaPi Fig. 4. The charge density measured is of 61.5 μC/cm^2. The only observed difference is the higher stability that supposes the small displacement of the potential (~30 mV) to more negative values for the later. The shorter chain length of the EG18 may be sufficient to avoid the effect of the excluded volume effect and the accumulation of water into the film is not produced as it happens with EG45 and EG136 molecules.

Another evidence of the different behavior of the RD of the EGn-SAMs as a function of the chain length formed in the absence and presence of NaPi is found from double layer capacitance curves (Fig. 5). The general pattern shown for these curves is the low and constant

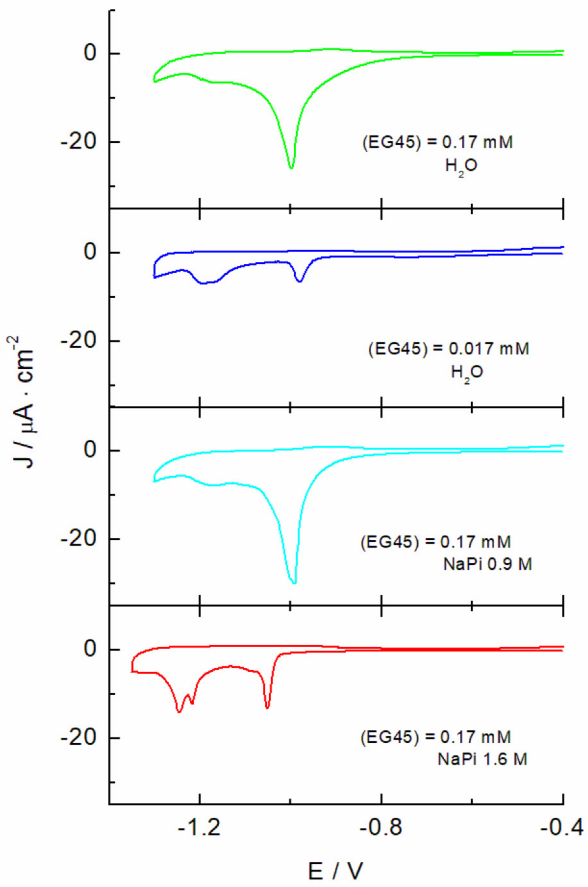

Fig. 3. CVs for the RD process of the EG45-SAM at PO electrodes formed in solutions of different EG45 concentrations and in the absence and presence of NaPi salt; v = 0.02 V/s.

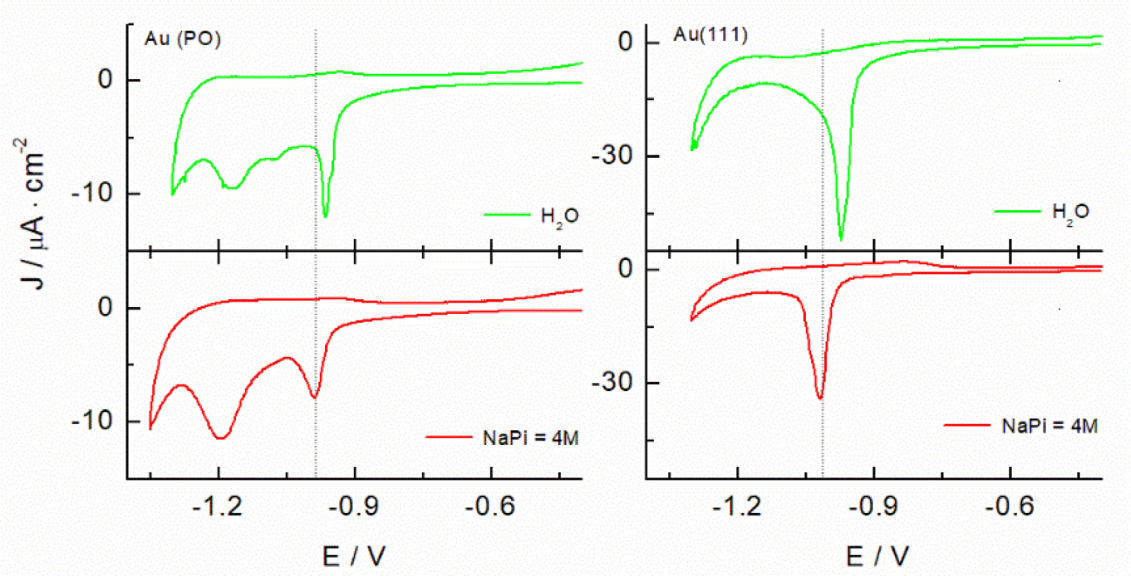

Fig. 4. CVs for the RD process of the EG18-SAM at Au(PO) and Au(1 1 1) electrodes formed in solutions of different NaPi salt concentrations. (EG18) = 0.18 mM; v = 0.02 V/s.

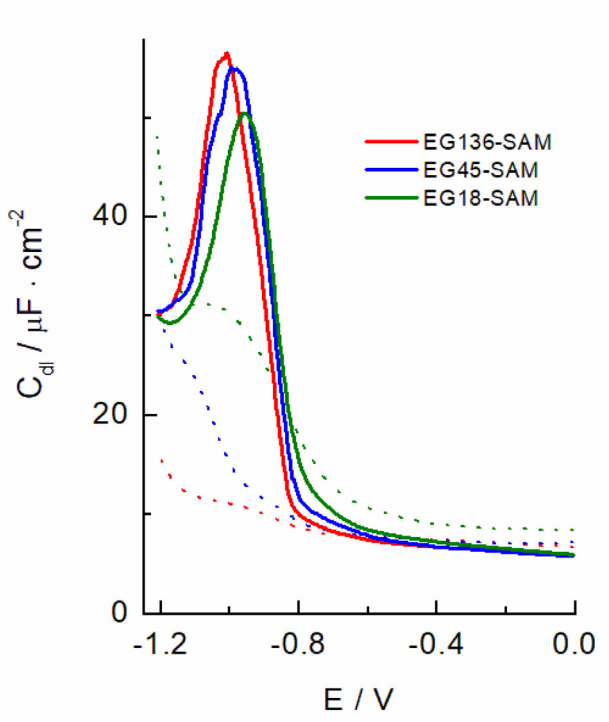

Fig. 5. Double layer capacity curves for the EGn-SAMs formed in EGn water (solid lines) or aqueous NaPi solutions (dashed lines) at the concentrations just below the cloud points (4 M for EG18, 1.6 M for EG45 and 0.9 M for EG136).

capacity value in the potential interval of SAM stability, indicating the existence of a compact layer that should behave as an ideal capacitor, followed for a hump coinciding with the potentials for SAM RD processes. It is interesting to observe that the peak recorded at lower potentials strongly differs from the SAMs prepared in pure water EGn solutions or in the presence of NaPi at concentrations just below the cloud point. This higher capacity signals should be correlated with the higher charge densities obtained in the voltammetric RD profiles for the SAMs formed in pure water solutions.

The charge densities obtained from the RD processes by using the cloud point grafting strategy can be used to get information about the surface coverage and conformation of the polymer SAMs. Table 1 gathers the grafting density values (σ) for the EG136-, EG45-, and EG18-SAMs obtained directly from the charge densities after correction of the capacitive contribution ($Q = nF\Gamma$, where Γ is the surface coverage of the SAM). In a recent study of the grafting density of EG113 by using surface plasmon resonance (SPR) measurements in the presence of various Na_2SO_4 salt concentrations, values ranging from 0.26 to 1.60 chains nm^{-2} have been obtained for the films formed in water and up to 0.6 M Na_2SO_4, respectively [21]. In that work, the importance of the modification time to obtain a high coverage is highlighted as deduced by comparison with other studies [13,17,19,22,50,51]. The methodologies used to build these EGn films include the use of changing temperature or the presence of different salt concentrations to reach the cloud point conditions as we have made in this work. However, the techniques used to obtain the grafting density values were SPR [19,21], X ray photoelectronic spectroscopy [51] and most of them, ellipsometry [13,17,22,50]. It seems that these techniques give lower coverage values that these obtained by electrochemical RD processes. However, if we compare the σ values obtained in the present work with those reported for gold nanoparticles (AuNPs) surfaces and determined by thermogravimetric analysis, we found a better correlation [52,53]. In fact, the size of the AuNPs used in these works are large and the system should behave close to a planar surface showing similar σ values [54,55].

Under the experimental conditions used to obtain the grafting densities of Table 1, i.e., cloudy point or θ-conditions, the theoretical values of the Flory radius, that gives the coil size of the polymer, can be determined by:

$$R_F = b\left(\frac{a \cdot N}{b}\right)^{1/2} \quad (1)$$

where a is the monomer size (a = 0.28 nm for polyethylene glycol in water) [56], b is the Kuhn length (b = 0.73) [21], and N is the number of monomer in the chain. The exponent *1/2* has been given for θ-solvent conditions. The distance between the center of grafting points in the surface is given by $P = (1/\sigma)^{1/2}$, and these values are much

Table 1
Molecular and conformational parameters of the EGn chains in the SAMs.

	σ / chains·nm^2	Footprint / Å^2	R_F / nm	H / nm	L / nm	(H/L)x100
EG136	2.25	44.4	5.27	28.0	38.1	73.6
EG45	2.30	43.5	3.03	9.35	12.1	73.4
EG18	3.07	32.6	1.92	4.12	5.1	81.7
EG7[(1)]	3.43	29.0	1.20	1.66	2.0	72.3

[(1)] Data taken from ref. [31].

lower than $2R_F$, leading us to conclude that the EGn chains are in an extended conformation forming a thick layer. By using the Alexander de Gennes scaling relation [14]:

$$H = \left(\frac{\sigma}{3}\right)^{1/3} \cdot b^{2/3} \cdot a \cdot N \quad (2)$$

the brush heights H can be found. The H values gathered in Table 1 would correspond to the EGn molecules exposed to a good solvent as it is the case. In fact, although the SAMs are formed under θ-conditions, the RD experiments are carried out in 0.1 M KOH solutions that would correspond to good solvent conditions. Thus, the equilibration of the EGn layers with this solution should lead to the elongation of the chains to be accommodated with the different environment. The obtained values, although higher than $2R_F$, account for the 70–80 % of the theoretical length for a helicoidal conformation of the chains, confirming this hypothesis.

Another interesting piece of information can be obtained by analyzing the blocking properties of these layers. It has been shown that the electrochemical signal of a redox species in solution is decreased when the electrode active area is either reduced or completely blocked as the approach of the species to the electrode surface is prevented [43,57]. The analysis of these signals is a good tool to determine the presence and nature of defects in the layers [58]. We have carried out cyclic voltammetric experiments of the $Fe(CN)_6^{3-/4-}$ redox pair as it has been shown to be very sensitive to the presence of EGn layers on electrodes [31].

As it is shown in Fig. 6, the redox response in cyclic voltammetry is completely suppressed when the gold electrode is covered by EG136-SAM formed either in water or in 0.9 M NaPi. The curves are typical of cases that involve a tunneling mechanism and, in a first approximation, would agree with the absence of defects or pinholes in the layers. However, electrochemical impedance spectroscopy is a more sensitive tool and allows the determination of the charge transfer resistance of the redox probe in the presence of the monolayer and thus, the surface coverage. The impedance signals obtained for the redox pair in the presence of EG136-SAM show, on one hand, the typical semicircle that indicates a high charge transfer resistance, and on the other, the absence of straight line at low frequencies showing the absence of diffusion of the redox pair to the electrode surface. It is observed that the semicircle diameter is higher for the SAM formed under conditions near the cloud point indicating higher compactness. A similar behavior is shown by the EG45- and EG18-SAMs, although in these cases the difference in the semicircle diameter is bigger, pointing to an even higher compactness of the layers formed under near cloud point conditions in respect to these formed in water.

The fitting of the spectra by using a Randle's equivalent circuit allows to determine the charge transfer resistance, R_{CT}. The R_{CT} can be related to the apparent surface coverage (θ) if we assume that electron transfer reactions occur only at the uncovered surface. Thus, the apparent fractional coverage of the electrode can be estimated by using equation (3) [57,59],

$$\theta = 1 - \left(\frac{R_{CT}^{bare}}{R_{CT}^{SAM}}\right) \quad (3)$$

where R_{CT}^{bare} is the value corresponding to the gold bare surface and R_{CT}^{SAM} these determined in the presence of the SAMs. The surfaces coverage values obtained are gathered in Table 2.

These apparent surface coverages indicate a strong blocking effect of the EGn-SAMs against the $Fe(CN)_6^{3-/4-}$ redox pair. Only in the case of the EG18-SAM and, in particular, when formed in a water solution, the presence of pinholes is presumed. This analysis allows us to conclude that the EGn layers, either formed in absence or presence of high salt concentrations, have compact structures and they don't present defects at least to be detected by the $Fe(CN)_6^{3-/4-}$ redox pair. The higher R_{CT} values measured for the SAMs formed under cloud point conditions would agree with the increased grafting density proposed in our model.

4. Conclusions

This work proposes a strategy to determine grafting densities of EGn molecules of different chain length by a simple experiment consisting in the analysis of the RD process of the SAM. The method uses the cloud point approach to build films in a brush conformation increasing in this way the grafting density of the SAMs. The high propensity of EGn chains to interact with water molecules provokes the formation of the films that contain a high ratio of water and present a mushroom conformation. The addition of high salt concentrations to the EGn solutions allows the shrinking of the chains and a better organization of the formed films. This phenomenon is clearly observed by comparing the RD profiles of the SAMs formed in the absence and presence of the salt at concentrations close to their cloud points and is confirmed by electrochemical impedance spectroscopy analyzing the behavior of the $Fe(CN)_6^{3-/4-}$ redox pair. This methodology then, serves to recognize the formation of the highly organized brush conformation by analyzing the shape of the cyclic voltammogram, and to determine a more realistic grafting density values than those reported in the literature by using ellipsometry [13,17,22,50] and surface plasmon resonance [19,21] techniques, within others. The procedure can be extended to other polymer chains of different chemical nature that can form SAMs on metal surfaces by the grafting to approach methodology.

CRediT authorship contribution statement

Miriam Chávez: Conceptualization, Methodology, Validation, Investigation. **Guadalupe Sánchez-Obrero:** Conceptualization, Methodology, Writing – review & editing. **Rafael Madueño:** Conceptualization, Methodology, Writing – review & editing. **José Manuel Sevilla:** Conceptualization, Methodology, Writing – review & editing. **Manuel Blázquez:** Conceptualization, Methodology, Writing – original draft, Writing – review & editing. **Teresa Pineda:** Conceptualization, Methodology, Writing – original draft, Writing – review & editing, Funding acquisition.

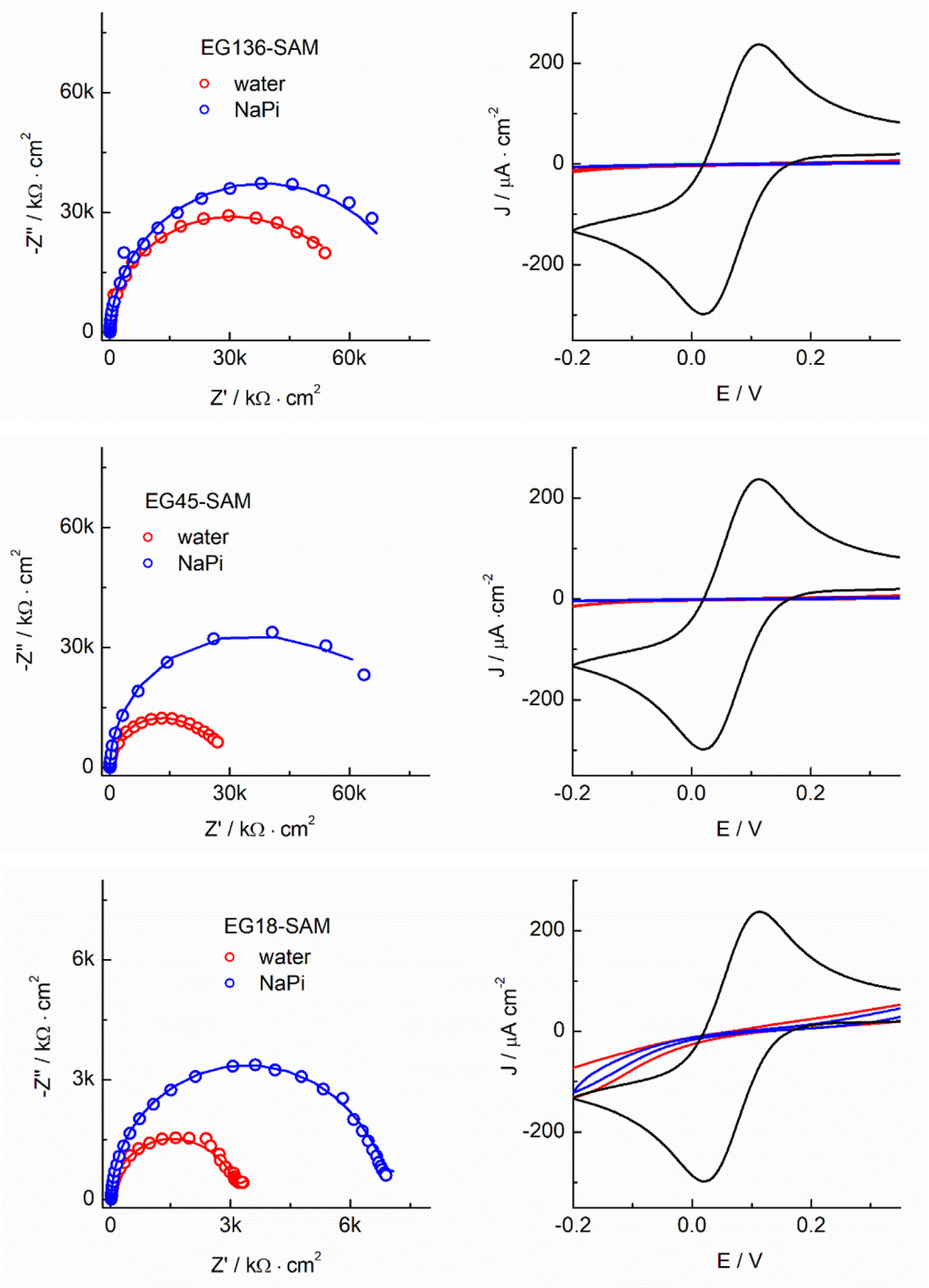

Fig. 6. Electrochemical response of the $Fe(CN)_6^{3-/4-}$ redox pair (1 mM in each component) in 0.1 M KNO_3 in the presence of EGn-SAMs formed in water (0.18 mM EGn) and/or 0.9 M NaPi forEG136; 1.6 M NaPi for EG45 and, 4 M NaPi for EG18. Left: Electrochemical impedance spectra. The circles are the experimental data and the lines are the results of the fitting analysis; Right: Cyclic voltammograms recorded at the scan rate of 0.1 V/s; the black line corresponds to the response at the bare electrode.

Table 2
Charge transfer resistances and apparent surface coverages estimated by eqn. (3) for the EGn-SAMs formed under different experimental conditions.

	R_{CT} / kΩ · cm²		Surface coverage, θ	
Formation media	**H_2O**	**NaPi**	**H_2O**	**NaPi**
EG136	268.9	320	0.9999	0.9999
EG45	114.6	282	0.9998	0.9999
EG18	16.6	31.7	0.9988	0.9993

Declaration of Competing Interest

The authors declare that they have no known competing financial interests or personal relationships that could have appeared to influence the work reported in this paper.

Acknowledgements

We thank the Ministerio de Ciencia e Innovación (Project RED2018-102412-T Network of Excellence Electrochemical Sensors and Biosensors), Junta de Andalucía and Universidad de Cordoba (UCO-FEDER-2018: ref. 1265074-2B and Plan Propio, Submod. 1.2. P.P. 2019) for financial support of this work. M.C. acknowledges Ministerio de Universidades for FPU 17/03873 grant.

Appendix A. Supplementary data

Supplementary data to this article can be found online at https://doi.org/10.1016/j.jelechem.2022.116294.

References

[1] A. Ulman, Formation and Structure of Self-Assembled Monolayers, Chem. Rev. (Washington, D. C.) 96(4) (1996) 1533-1554.
[2] J.C. Love, L.A. Estroff, J.K. Kriebel, R.G. Nuzzo, G.M. Whitesides, Self-Assembled Monolayers of Thiolates on Metals as a Form of Nanotechnology, Chem. Rev. 105 (4) (2005) 1103–1169.
[3] P.S. Weiss, Functional Molecules and Assemblies in Controlled Environments: Formation and Measurements, Acc. Chem. Res. 41 (12) (2008) 1772–1781.
[4] J.E. Raynor, J.R. Capadona, D.M. Collard, T.A. Petrie, A.J. Garcia, Polymer brushes and self-assembled monolayers: Versatile platforms to control cell adhesion to biomaterials (review), Biointerphases 4 (2) (2009) FA3-FA16.
[5] A.S. Karakoti, S. Das, S. Thevuthasan, S. Seal, PEGylated Inorganic Nanoparticles, Angew. Chem. Int. Ed. 50 (9) (2011) 1980–1994.
[6] R.L.C. Wang, H.J. Kreuzer, M. Grunze, Molecular conformation and solvation of oligo(ethylene glycol)-terminated self-assembled monolayers and their resistance to protein adsorption, J. Phys. Chem. B 101 (47) (1997) 9767–9773.
[7] P. Harder, M. Grunze, R. Dahint, G.M. Whitesides, P.E. Laibinis, Molecular conformation in oligo(ethylene glycol)-terminated self-assembled monolayers on gold and silver surfaces determines their ability to resist protein adsorption, J. Phys. Chem. B 102 (2) (1998) 426–436.
[8] S. Tokumitsu, A. Liebich, S. Herrwerth, W. Eck, M. Himmelhaus, M. Grunze, Grafting of alkanethiol-terminated poly(ethylene glycol) on gold, Langmuir 18 (23) (2002) 8862–8870.
[9] S. Herrwerth, W. Eck, S. Reinhardt, M. Grunze, Factors that determine the protein resistance of oligoether self-assembled monolayers - Internal hydrophilicity, terminal hydrophilicity, and lateral packing density, J. Am. Chem. Soc. 125 (31) (2003) 9359–9366.
[10] J. Fick, R. Steitz, V. Leiner, S. Tokumitsu, M. Himmelhaus, M. Grunze, Swelling behavior of self-assembled monolayers of alkanethiol-terminated poly(ethylene glycol): A neutron reflectometry study, Langmuir 20 (10) (2004) 3848–3853.
[11] M.W.A. Skoda, F. Schreiber, R.A.J. Jacobs, J.R.P. Webster, M. Wolff, R. Dahint, D. Schwendel, M. Grunze, Protein Density Profile at the Interface of Water with Oligo (ethylene glycol) Self-Assembled Monolayers, Langmuir 25 (7) (2009) 4056–4064.
[12] U.R. Dahal, Z. Wang, E.E. Dormidontova, Hydration and Mobility of Poly(ethylene oxide) Brushes, Macromolecules 50 (17) (2017) 6722–6732.
[13] L.D. Unsworth, Z. Tun, H. Sheardown, J.L. Brash, Chemisorption of thiolated poly (ethylene oxide) to gold: surface chain densities measured by ellipsometry and neutron reflectometry, J. Colloid Interf. Sci. 281 (1) (2005) 112–121.
[14] P.G. de Gennes, Conformations of Polymers Attached to an Interface, Macromolecules 13 (5) (1980) 1069–1075.
[15] P.G. de Gennes, Polymers at an interface; a simplified view, Adv. Colloid Interf. Sci. 27 (3) (1987) 189–209.
[16] P. Kingshott, H. Thissen, H.J. Griesser, Effects of cloud-point grafting, chain length, and density of PEG layers on competitive adsorption of ocular proteins, Biomaterials 23 (9) (2002) 2043–2056.
[17] W. Taylor, R.A.L. Jones, Producing High-Density High-Molecular-Weight Polymer Brushes by a "Grafting to" Method from a Concentrated Homopolymer Solution, Langmuir 26 (17) (2010) 13954–13958.
[18] W. Taylor, R.A.L. Jones, Protein Adsorption on Well-Characterized Polyethylene Oxide Brushes on Gold: Dependence on Molecular Weight and Grafting Density, Langmuir 29 (20) (2013) 6116–6122.
[19] G. Emilsson, R.L. Schoch, L. Feuz, F. Höök, R.Y.H. Lim, A.B. Dahlin, Strongly Stretched Protein Resistant Poly(ethylene glycol) Brushes Prepared by Grafting-To, ACS Appl. Mater. Interfaces 7 (14) (2015) 7505–7515.
[20] S.T. Milner, Polymer Brushes, Science 251 (4996) (1991) 905.
[21] R. Ortiz, S. Olsen, E. Thormann, Salt-Induced Control of the Grafting Density in Poly(ethylene glycol) Brush Layers by a Grafting-to Approach, Langmuir 34 (15) (2018) 4455–4464.
[22] L.D. Unsworth, H. Sheardown, J.L. Brash, Protein-Resistant Poly(ethylene oxide)-Grafted Surfaces: Chain Density-Dependent Multiple Mechanisms of Action, Langmuir 24 (5) (2008) 1924–1929.
[23] T. Laredo, J. Leitch, M. Chen, I.J. Burgess, J.R. Dutcher, J. Lipkowski, Measurement of the Charge Number Per Adsorbed Molecule and Packing Densities of Self-Assembled Long-Chain Monolayers of Thiols, Langmuir 23 (11) (2007) 6205–6211.
[24] I. Thom, M. Buck, On the interpretation of multiple waves in cyclic voltammograms of self-assembled monolayers of n-alkane thiols on gold, Z. Phys. Chem. 222 (5–6) (2008) 739–754.
[25] C.A. Widrig, C. Chung, M.D. Porter, The electrochemical desorption of n-alkanethiol monolayers from polycrystalline gold and silver electrodes, J. Electroanal. Chem. 310 (1–2) (1991) 335–359.
[26] D.W. Hatchett, R.H. Uibel, K.J. Stevenson, J.M. Harris, H.S. White, Electrochemical measurement of the free energy of adsorption of n-alkanethiolates at Ag(111), J. Am. Chem. Soc. 120 (5) (1998) 1062–1069.
[27] D.F. Yang, C.P. Wilde, M. Morin, Electrochemical desorption and adsorption of nonyl mercaptan at gold single crystal electrode surfaces, Langmuir 12 (26) (1996) 6570–6577.
[28] D.F. Yang, C.P. Wilde, M. Morin, Studies of the electrochemical removal and efficient re-formation of a monolayer of hexadecanethiol self-assembled at an Au (111) single crystal in aqueous solutions, Langmuir 13 (2) (1997) 243–249.
[29] T. Kakiuchi, H. Usui, D. Hobara, M. Yamamoto, Voltammetric Properties of the Reductive Desorption of Alkanethiol Self-Assembled Monolayers from a Metal Surface, Langmuir 18 (13) (2002) 5231–5238.
[30] R. Madueno, J.M. Sevilla, T. Pineda, A.J. Roman, M. Blazquez, A voltammetric study of 6-mercaptopurine monolayers on polycrystalline gold electrodes, J. Electroanal. Chem. 506 (2) (2001) 92–98.
[31] M. Chávez, G. Sánchez-Obrero, R. Madueño, J.M. Sevilla, M. Blázquez, T. Pineda, Characterization of a self-assembled monolayer of O-(2-Mercaptoethyl)-O′-methyl-hexa(ethylene glycol) (EG7-SAM) on gold electrodes, J. Electroanal. Chem. 880 (2021) 114892.
[32] T. Doneux, M. Steichen, A. De Rache, C. Buess-Herman, Influence of the crystallographic orientation on the reductive desorption of self-assembled monolayers on gold electrodes, J. Electroanal. Chem. 649 (1–2) (2010) 164–170.
[33] S.S. Wong, M.D. Porter, Origin of the multiple voltammetric desorption waves of long-chain alkanethiolate monolayers chemisorbed on annealed gold electrodes, J. Electroanal. Chem. 485 (2) (2000) 135–143.
[34] M.M. Walczak, C.A. Alves, B.D. Lamp, M.D. Porter, Electrochemical and X-ray photoelectron spectroscopic evidence for differences in the binding sites of alkanethiolate monolayers chemisorbed at gold, J. Electroanal. Chem. 396 (1–2) (1995) 103–114.
[35] C.J. Zhong, M.D. Porter, Fine structure in the voltammetric desorption curves of alkanethiolate monolayers chemisorbed at gold, Journal of Electroanalytical Chemistry 425 (1–2) (1997) 147–153.
[36] C.J. Zhong, J. Zak, M.D. Porter, Voltammetric reductive desorption characteristics of alkanethiolate monolayers at single crystal Au(111) and (110) electrode surfaces, J. Electroanal. Chem. 421 (1–2) (1997) 9–13.
[37] M. Byloos, H. Al-Maznai, M. Morin, Formation of a Self-Assembled Monolayer via the Electrospreading of Physisorbed Micelles of Thiolates, J. Phys. Chem. B 103 (31) (1999) 6554–6561.
[38] D.F. Yang, H. AlMaznai, M. Morin, Vibrational study of the fast reductive and the slow oxidative desorptions of a nonanethiol self-assembled monolayer from a Au (111) single crystal electrode, J. Phys. Chem. B 101 (7) (1997) 1158–1166.
[39] M.M. Walczak, D.D. Popenoe, R.S. Deinhammer, B.D. Lamp, C.K. Chung, M.D. Porter, Reductive Desorption of Alkanethiolate Monolayers at Gold - A Measure of Surface Coverage, Langmuir 7 (11) (1991) 2687–2693.
[40] G. Sanchez-Obrero, M. Chavez, R. Madueno, M. Blazquez, T. Pineda, J.M. Lopez-Romero, F. Sarabia, J. Hierrezuelo, R. Contreras-Caceres, Study of the self-assembly process of an oligo(ethylene glycol)-thioacetyl substituted theophylline (THEO) on gold substrates, J. Electroanal. Chem. 823 (2018) 663–671.
[41] M.L. Carot, M.J. Esplandiu, F.P. Cometto, E.M. Patrito, V.A. Macagno, Reactivity of 1,8-octanedithiol monolayers on Au(1 1 1): Experimental and theoretical investigation, J. Electroanal. Chem. 579 (1) (2005) 13–23.
[42] M.J. Esplandiu, H. Hagenstrom, D.M. Kolb, Functionalized Self-Assembled Alkanethiol Monolayers on Au(111) Electrodes: 1, Surface Structure and Electrochemistry, Langmuir 17 (3) (2001) 828–838.
[43] D. Garcia-Raya, R. Madueno, J. Manuel Sevilla, M. Blazquez, T. Pineda, Electrochemical characterization of a 1,8-octanedithiol self-assembled monolayer (ODT-SAM) on a Au(111) single crystal electrode, Electrochim. Acta 53 (27) (2008) 8026–8033.
[44] M.I. Muglali, A. Bashir, A. Terfort, M. Rohwerder, Electrochemical investigations on stability and protonation behavior of pyridine-terminated aromatic self-assembled monolayers, Phys. Chem. Chem. Phys. 13 (34) (2011) 15530–15538.
[45] M.I. Muglali, A. Erbe, Y. Chen, C. Barth, P. Koelsch, M. Rohwerder, Modulation of electrochemical hydrogen evolution rate by araliphatic thiol monolayers on gold, Electrochim. Acta 90 (2013) 17–26.
[46] Y.-T. Long, H.-T. Rong, M. Buck, M. Grunze, Odd–even effects in the cyclic voltammetry of self-assembled monolayers of biphenyl based thiols, J. Electroanal. Chem. 524–525 (2002) 62–67.
[47] T. Kawaguchi, H. Yasuda, K. Shimazu, M.D. Porter, Electrochemical Quartz Crystal Microbalance Investigation of the Reductive Desorption of Self-Assembled Monolayers of Alkanethiols and Mercaptoalkanoic Acids on Au, Langmuir 16 (25) (2000) 9830–9840.
[48] T.W. Schneider, D.A. Buttry, Electrochemical quartz crystal microbalance studies of adsorption and desorption of self-assembled monolayers of alkyl thiols on gold, J. Am. Chem. Soc. 115 (26) (1993) 12391–12397.
[49] S. Alexander, Adsorption of chain molecules with a polar head a scaling description, J. Phys. France 38 (8) (1977) 983–987.

[50] D.F. Marruecos, M. Kastantin, D.K. Schwartz, J.L. Kaar, Dense Poly(ethylene glycol) Brushes Reduce Adsorption and Stabilize the Unfolded Conformation of Fibronectin, Biomacromolecules 17 (3) (2016) 1017–1025.
[51] R. Ogaki, O.Z. Andersen, G.V. Jensen, K. Kolind, D.C.E. Kraft, J.S. Pedersen, M. Foss, Temperature-Induced Ultradense PEG Polyelectrolyte Surface Grafting Provides Effective Long-Term Bioresistance against Mammalian Cells, Serum, and Whole Blood, Biomacromolecules 13 (11) (2012) 3668–3677.
[52] M. Chavez, A. Fernandez-Merino, G. Sanchez-Obrero, R. Madueno, J.M. Sevilla, M. Blazquez, T. Pineda, Distinct thermoresponsive behaviour of oligo- and poly-ethylene glycol protected gold nanoparticles in concentrated salt solutions, Nanoscale Adv. 3 (16) (2021) 4767–4779.
[53] K. Rahme, L. Chen, R.G. Hobbs, M.A. Morris, C. O'Driscoll, J.D. Holmes, PEGylated gold nanoparticles: polymer quantification as a function of PEG lengths and nanoparticle dimensions, RSC Adv. 3 (17) (2013) 6085–6094.
[54] A. Jimenez, A. Sarsa, M. Blazquez, T. Pineda, A Molecular Dynamics Study of the Surfactant Surface Density of Alkanethiol Self-Assembled Monolayers on Gold Nanoparticles as a Function of the Radius, J. Phys. Chem. C 114 (49) (2010) 21309–21314.
[55] E. Reyes, R. Madueño, M. Blazquez, T. Pineda, Facile Exchange of Ligands on the 6-Mercaptopurine-Monolayer Protected Gold Clusters Surface, J. Phys. Chem. C 114 (38) (2010) 15955–15962.
[56] F. Oesterhelt, M. Rief, H.E. Gaub, Single molecule force spectroscopy by AFM indicates helical structure of poly(ethylene-glycol) in water, New Journal of Physics 1 (1999).
[57] H.O. Finklea, D.A. Snider, J. Fedyk, E. Sabatani, Y. Gafni, I. Rubinstein, Characterization of Octadecanethiol-Coated Gold Electrodes as Microarray Electrodes by Cyclic Voltammetry and Ac-Impedance Spectroscopy, Langmuir 9 (12) (1993) 3660–3667.
[58] H.O. Finklea, S. Avery, M. Lynch, T. Furtsch, Blocking oriented monolayers of alkyl mercaptans on gold electrodes, Langmuir 3 (3) (1987) 409–413.
[59] R.P. Janek, W.R. Fawcett, A. Ulman, Impedance Spectroscopy of Self-Assembled Monolayers on Au(111): Sodium Ferrocyanide Charge Transfer at Modified Electrodes, Langmuir 14 (11) (1998) 3011–3018.